

Stop quark searches at the LHC with boosted tops and transverse variables.

Works done in association with D.K. Ghosh, D. Ghosh, A. Chakraborty.
arXiv:1303.5776. JHEP 1310 (2013) 122.

Dipan Sengupta

Theoretical Physics Department, LPSC, Grenoble

April 16, 2014

- Although the Higgs has been found, deficiencies of the SM like hierarchy problem, absence of DM candidate,... force us to look beyond SM.
- SUSY has been the most sought after BSM for over 3 decades.

- Although the Higgs has been found, deficiencies of the SM like hierarchy problem, absence of DM candidate,... force us to look beyond SM.
- SUSY has been the most sought after BSM for over 3 decades.

	Superfield	Particle	Spin	Superpartner	Spin
Matter Fields	Q	$(u, d)_L$	$\frac{1}{2}$	$(\tilde{u}_L, \tilde{d}_L)$	0
	U^c	\bar{u}_R	$\frac{1}{2}$	\tilde{u}_R^*	0
	D^c	\bar{d}_R	$\frac{1}{2}$	\tilde{d}_R^*	0
	L	$(\nu, e)_L$	$\frac{1}{2}$	$(\tilde{\nu}_L, \tilde{e}_L)$	0
	E^c	\bar{e}_R	$\frac{1}{2}$	\tilde{e}_R^*	0
Gauge Fields	V_1	B_μ	1	\tilde{B}	$\frac{1}{2}$
	V_2	W_μ^i	1	\tilde{W}^i	$\frac{1}{2}$
	V_3	G_μ^a	1	\tilde{g}^a	$\frac{1}{2}$
Higgs Fields	H_1	(H_1^0, H_1^-)	0	$(\tilde{H}_1^0, \tilde{H}_1^-)$	$\frac{1}{2}$
	H_2	(H_2^+, H_2^0)	0	$(\tilde{H}_2^+, \tilde{H}_2^0)$	$\frac{1}{2}$

Table: MSSM particle content.

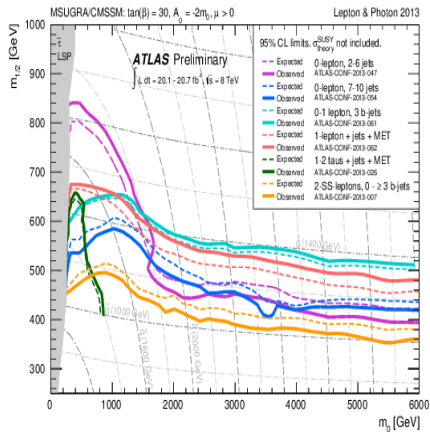
- Although the Higgs has been found, deficiencies of the SM like hierarchy problem, absence of DM candidate,... force us to look beyond SM.
- SUSY has been the most sought after BSM for over 3 decades.

	Superfield	Particle	Spin	Superpartner	Spin
Matter Fields	Q	$(u, d)_L$	$\frac{1}{2}$	$(\tilde{u}_L, \tilde{d}_L)$	0
	U^c	\bar{u}_R	$\frac{1}{2}$	\tilde{u}_R^*	0
	D^c	\bar{d}_R	$\frac{1}{2}$	\tilde{d}_R^*	0
	L	$(\nu, e)_L$	$\frac{1}{2}$	$(\tilde{\nu}_L, \tilde{e}_L)$	0
	E^c	\bar{e}_R	$\frac{1}{2}$	\tilde{e}_R^*	0
Gauge Fields	V_1	B_μ	1	\tilde{B}	$\frac{1}{2}$
	V_2	W_μ^i	1	\tilde{W}^i	$\frac{1}{2}$
	V_3	G_μ^a	1	\tilde{g}^a	$\frac{1}{2}$
Higgs Fields	H_1	(H_1^0, H_1^-)	0	$(\tilde{H}_1^0, \tilde{H}_1^-)$	$\frac{1}{2}$
	H_2	(H_2^+, H_2^0)	0	$(\tilde{H}_2^+, \tilde{H}_2^0)$	$\frac{1}{2}$

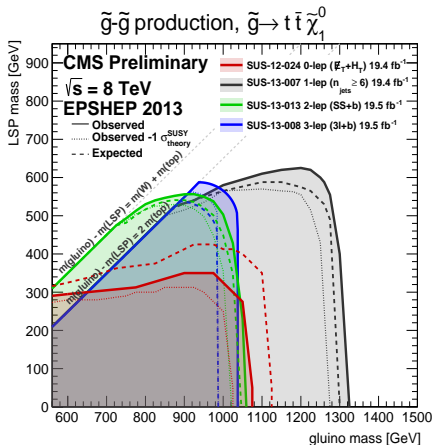
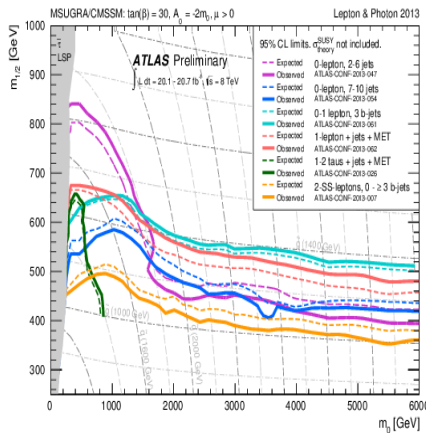
Table: MSSM particle content.

- Early SUSY searches relied on specific models of SUSY breaking scenarios, in particular CMSSM/mSUGRA.
- However absence of SUSY signatures have prompted a more generic approach.

CMSSM: Specified by 4 parameters and a sign at GUT scale. $m_0, m_{1/2}, \tan\beta, A_0, \text{sgn}(\mu)$



CMSSM: Specified by 4 parameters and a sign at GUT scale. $m_0, m_{1/2}, \tan\beta, A_0, \text{sgn}(\mu)$



$$m_{\tilde{g}} \simeq m_{\tilde{q}} \simeq 1.6 \text{ TeV}, m_{\tilde{g}} \ll m_{\tilde{q}} \simeq 1.4 \text{ TeV}$$

- In the absence of a signal for the gluino and 1st two generation squarks, attention has turned to 3rd generation.

The Stop sector of SUSY

- In the absence of a signal for the gluino and 1st two generation squarks, attention has turned to 3rd generation.

$$M_{\tilde{f}}^2 = \begin{pmatrix} M_{\tilde{f}_{LL}}^2 & M_{\tilde{f}_{LR}}^2 \\ M_{\tilde{f}_{RL}}^2 & M_{\tilde{f}_{RR}}^2 \end{pmatrix}.$$

- Third Generation : Large mixings, resulting in a splitting in third generation mass eigen states.

$$\begin{pmatrix} \tilde{t}_1 \\ \tilde{t}_2 \end{pmatrix} = \begin{pmatrix} m_{\tilde{q}_3}^2 + (1/2 - 2/3 \sin^2 \theta_w) M_Z^2 \cos 2\beta + m_t^2 & -m_t(A_t^* - \mu \cot \beta) \\ -m_t(A_t - \mu^* \cot \beta) & m_{\tilde{t}}^2 + 2/3 \sin^2 \theta_w M_Z^2 \cos 2\beta + m_t^2 \end{pmatrix} \begin{pmatrix} \tilde{t}_L \\ \tilde{t}_R \end{pmatrix}$$

$$(m_{\tilde{t}_1, \tilde{t}_2})^2 = \frac{1}{2} \left\{ m_{\tilde{t}_L}^2 + m_{\tilde{t}_R}^2 \pm \sqrt{[(m_{\tilde{t}_L}^2 - m_{\tilde{t}_R}^2)^2 + 4X_t^2 m_t^2]} \right\}$$

$$X_t = A_t - \mu \cot \beta$$

- Intimately Connected to the Higgs loop correction.

- Reason 1: We have not found any SUSY signature for the gluino and the 1st two generation squarks

- Reason 1: We have not found any SUSY signature for the gluino and the 1st two generation squarks
- Reason 2 : Naturalness requirements. Cancellation of quadratic divergences predominantly through stops.

- Reason 1: We have not found any SUSY signature for the gluino and the 1st two generation squarks
- Reason 2 : Naturalness requirements. Cancellation of quadratic divergences predominantly through stops.
- Reason 3 : Principal loop contributor to the increase of Higgs mass
- Lightest Higgs mass : $m_h^2 \leq m_Z^2 \cos^2 2\beta \leq 90 \text{ GeV}$
- Loop Corrections : dominated by top-stop loops:

$$\delta m_h^2 = \frac{3G_F}{\sqrt{2}\pi^2} m_t^4 \left[\log \frac{M_{SUSY}^2}{m_t^2} + \left(\frac{X_t^2}{M_{SUSY}^2} \left(1 - \frac{X_t^2}{12M_{SUSY}^2} \right) \right) \right] \leq 135 \text{ GeV}$$

$$X_t = A_t - \mu \cot \beta. \quad M_{SUSY} = \sqrt{\tilde{t}_1 \tilde{t}_2}$$

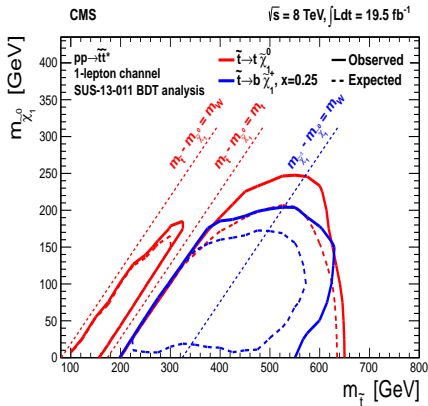
- Reason 1: We have not found any SUSY signature for the gluino and the 1st two generation squarks
- Reason 2 : Naturalness requirements. Cancellation of quadratic divergences predominantly through stops.
- Reason 3 : Principal loop contributor to the increase of Higgs mass
- Lightest Higgs mass : $m_h^2 \leq m_Z^2 \cos^2 2\beta \leq 90 \text{ GeV}^2$
- Loop Corrections : dominated by top-stop loops:

$$\delta m_h^2 = \frac{3G_F}{\sqrt{2}\pi^2} m_t^4 \left[\log \frac{M_{SUSY}^2}{m_t^2} + \left(\frac{X_t^2}{M_{SUSY}^2} \left(1 - \frac{X_t^2}{12M_{SUSY}^2} \right) \right) \right] \leq 135 \text{ GeV}^2$$

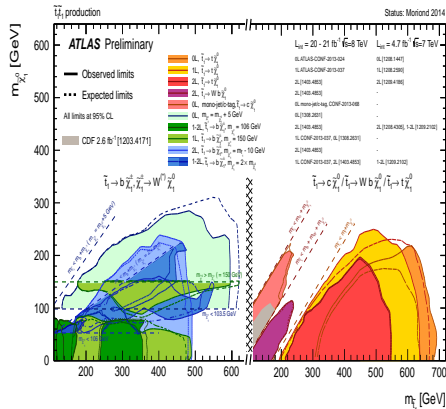
$$X_t = A_t - \mu \cot \beta. \quad M_{SUSY} = \sqrt{\tilde{t}_1 \tilde{t}_2}$$

- **tops squarks : below 500–1000 GeV**
- **Lighter Chargino and two lighter neutralinos: 200–450 GeV**
- **A Not too heavy Gluino 1–1.5 TeV**

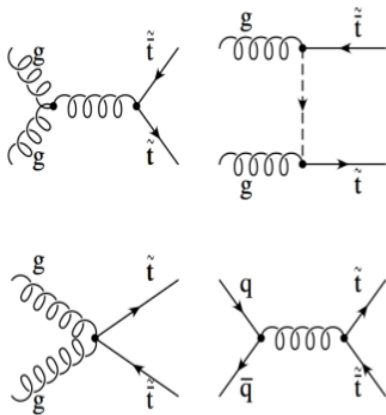
Limits on stop masses: CMS and ATLAS



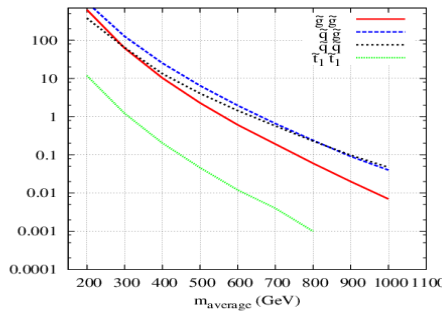
$$m_{\tilde{t}_1} = 600, m_{\tilde{\chi}_1^0} = 250 \text{ GeV}, \tilde{t} \rightarrow t \tilde{\chi}_1^0.$$



Production modes, Cross Section at 8 TeV



C.S (pb)



The parameter spaces of interest

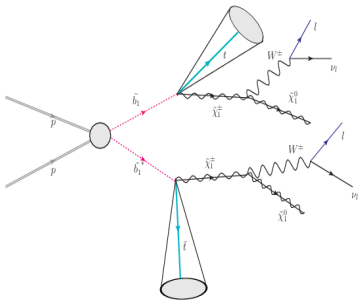
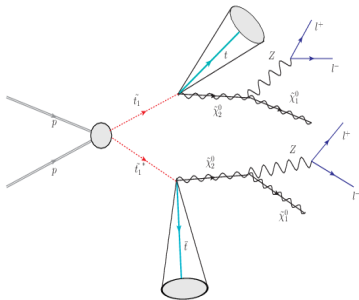
- Most of the early stop searches assumed simplified models with $\tilde{t}_1 \rightarrow t\chi_1^0$. **Predominantly right handed stops.**
- Efficiency dependent on $\Delta m = m_{\tilde{t}_1} - m_{\chi_1^0}$. Kinematic edges difficult to probe due to large $t\bar{t}$ background.

The parameter spaces of interest

- Most of the early stop searches assumed simplified models with $\tilde{t}_1 \rightarrow t\chi_1^0$. **Predominantly right handed stops.**
- Efficiency dependent on $\Delta m = m_{\tilde{t}_1} - m_{\chi_1^0}$. Kinematic edges difficult to probe due to large $t\bar{t}$ background.
- However left handed stops are also a possibility, and final states are rich in jet/leptonic activity.
- In the context of simplified models, PMSSM framework the left handed nature of stops/sbottoms is important.

The parameter spaces of interest

- Most of the early stop searches assumed simplified models with $\tilde{t}_1 \rightarrow t\chi_1^0$. **Predominantly right handed stops.**
- Efficiency dependent on $\Delta m = m_{\tilde{t}_1} - m_{\chi_1^0}$. Kinematic edges difficult to probe due to large $t\bar{t}$ background.
- However left handed stops are also a possibility, and final states are rich in jet/leptonic activity.
- In the context of simplified models, PMSSM framework the left handed nature of stops/sbottoms is important.



Signature and benchmark points

$$\begin{aligned}
 \text{pp} &\rightarrow \tilde{t}_1 \tilde{t}_1^* \rightarrow t \bar{t} \tilde{\chi}_2^0 \tilde{\chi}_2^0 \rightarrow t \bar{t} + 2Z + 2\tilde{\chi}_1^0 \rightarrow t/\bar{t} + \ell\ell + \cancel{p}_T + X \\
 \text{pp} &\rightarrow \tilde{t}_1 \tilde{t}_1^* \rightarrow t \bar{b} \tilde{\chi}_2^0 \tilde{\chi}_1^- \rightarrow t \bar{b} + W^- Z + 2\tilde{\chi}_1^0 \rightarrow t + \ell\ell + \cancel{p}_T + X \\
 \text{pp} &\rightarrow \tilde{t}_1 \tilde{t}_1^* \rightarrow t \bar{b} \tilde{\chi}_2^0 \tilde{\chi}_1^- \rightarrow t \bar{b} + W^- h + 2\tilde{\chi}_1^0 \rightarrow t + \ell\ell + \cancel{p}_T + X \\
 \text{pp} &\rightarrow \tilde{b}_1 \tilde{b}_1^* \rightarrow t \bar{t} \tilde{\chi}_1^+ \tilde{\chi}_1^- \rightarrow t \bar{t} + W^+ W^- + 2\tilde{\chi}_1^0 \rightarrow t/\bar{t} + \ell\ell + \cancel{p}_T + X \\
 \text{pp} &\rightarrow \tilde{b}_1 \tilde{b}_1^* \rightarrow t \bar{b} \tilde{\chi}_1^- \tilde{\chi}_2^0 \rightarrow t \bar{b} + W^- Z + 2\tilde{\chi}_1^0 \rightarrow t + \ell\ell + \cancel{p}_T + X.
 \end{aligned}$$

	P1	P2	P3	P4	P5	P6
m_{Q_3}	500	500	700	700	900	900
$m_{\tilde{t}_1}$	501.7	501.7	714.2	714.2	918.1	918.1
$m_{\tilde{b}_1}$	525.4	525.4	748.4	748.4	918.1	918.1
$m_{\tilde{\chi}_1^0}$	48.5	97.9	146.3	97.8	149.0	198.3
$m_{\tilde{\chi}_2^0}$	193.3	193.9	245.9	244.3	297.9	298.6
$m_{\tilde{\chi}_1^\pm}$	192.8	192.8	242.7	242.7	297.0	297.0
$\text{BR}(\tilde{b}_1 \rightarrow b \tilde{\chi}_{2,3,4}^0)(\%)$	34.6	34.5	19.3	19.4	19.4	19.4
$\text{BR}(\tilde{b}_1 \rightarrow t \tilde{\chi}_{1,2}^\pm)(\%)$	65.4	65.5	80.7	80.6	80.6	80.6
$\text{BR}(\tilde{t}_1 \rightarrow t \tilde{\chi}_{2,3,4}^0)(\%)$	34.9	35.2	62.5	62.4	62.5	62.5
$\text{BR}(\tilde{t}_1 \rightarrow b \tilde{\chi}_{1,2}^\pm)(\%)$	65.1	64.8	37.5	37.6	37.5	37.5
$\text{BR}(\tilde{\chi}_2^0 \rightarrow \tilde{\chi}_1^0 Z)(\%)$	33.9	100.0	100.0	22.1	12.8	100.0
$\text{BR}(\tilde{\chi}_2^0 \rightarrow \tilde{\chi}_1^0 h)(\%)$	66.1	0.0	0.0	77.9	87.2	0.0

The rest of the parameter space is irrelevant for this study, and is decoupled from this set.

$$\begin{array}{llllllll}
 pp & \rightarrow & \tilde{t}_1 \tilde{t}_1^* & \rightarrow & t \bar{t} \tilde{\chi}_2^0 \tilde{\chi}_2^0 & \rightarrow & t \bar{t} + 2Z + 2\tilde{\chi}_1^0 & \rightarrow & t/\bar{t} + \ell\ell + \cancel{p}_T + X \\
 pp & \rightarrow & \tilde{t}_1 \tilde{t}_1^* & \rightarrow & t \bar{b} \tilde{\chi}_2^0 \tilde{\chi}_1^- & \rightarrow & t \bar{b} + W^- Z + 2\tilde{\chi}_1^0 & \rightarrow & t + \ell\ell + \cancel{p}_T + X \\
 pp & \rightarrow & \tilde{t}_1 \tilde{t}_1^* & \rightarrow & t \bar{b} \tilde{\chi}_2^0 \tilde{\chi}_1^- & \rightarrow & t \bar{b} + W^- h + 2\tilde{\chi}_1^0 & \rightarrow & t + \ell\ell + \cancel{p}_T + X \\
 pp & \rightarrow & \tilde{b}_1 \tilde{b}_1^* & \rightarrow & t \bar{t} \tilde{\chi}_1^+ \tilde{\chi}_1^- & \rightarrow & t \bar{t} + W^+ W^- + 2\chi_1^0 & \rightarrow & t/\bar{t} + \ell\ell + \cancel{p}_T + X \\
 pp & \rightarrow & \tilde{b}_1 \tilde{b}_1^* & \rightarrow & t \bar{b} \tilde{\chi}_1^- \chi_2^0 & \rightarrow & t \bar{b} + W^- Z + 2\chi_1^0 & \rightarrow & t + \ell\ell + \cancel{p}_T + X.
 \end{array}$$

- Signature of interest: 1 tagged top + di-lepton + jets + \cancel{p}_T at 14 TeV LHC.
- For 8 TeV, small cross sections, absence of boost are limiting factors to this analysis.

$$\begin{array}{llllll}
 pp & \rightarrow & \tilde{t}_1 \tilde{t}_1^* & \rightarrow & t \bar{t} \tilde{\chi}_2^0 \tilde{\chi}_2^0 & \rightarrow & t \bar{t} + 2Z + 2\tilde{\chi}_1^0 & \rightarrow & t/\bar{t} + \ell\ell + \cancel{p}_T + X \\
 pp & \rightarrow & \tilde{t}_1 \tilde{t}_1^* & \rightarrow & t \bar{b} \tilde{\chi}_2^0 \tilde{\chi}_1^- & \rightarrow & t \bar{b} + W^- Z + 2\tilde{\chi}_1^0 & \rightarrow & t + \ell\ell + \cancel{p}_T + X \\
 pp & \rightarrow & \tilde{t}_1 \tilde{t}_1^* & \rightarrow & t \bar{b} \tilde{\chi}_2^0 \tilde{\chi}_1^- & \rightarrow & t \bar{b} + W^- h + 2\tilde{\chi}_1^0 & \rightarrow & t + \ell\ell + \cancel{p}_T + X \\
 pp & \rightarrow & \tilde{b}_1 \tilde{b}_1^* & \rightarrow & t \bar{t} \tilde{\chi}_1^+ \tilde{\chi}_1^- & \rightarrow & t \bar{t} + W^+ W^- + 2\chi_1^0 & \rightarrow & t/\bar{t} + \ell\ell + \cancel{p}_T + X \\
 pp & \rightarrow & \tilde{b}_1 \tilde{b}_1^* & \rightarrow & t \bar{b} \tilde{\chi}_1^- \chi_2^0 & \rightarrow & t \bar{b} + W^- Z + 2\chi_1^0 & \rightarrow & t + \ell\ell + \cancel{p}_T + X.
 \end{array}$$

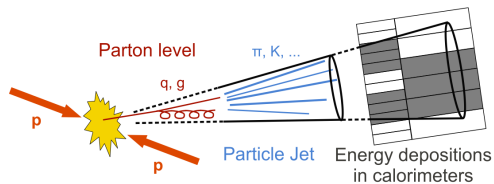
- Signature of interest: 1 tagged top + di-lepton + jets + \cancel{p}_T at 14 TeV LHC.
- For 8 TeV, small cross sections, absence of boost are limiting factors to this analysis.
- For this analysis, we use MADGRAPH to generate events, PYTHIA to shower and hadronize, FASTJET to reconstruct normal jets/Fat jets and Delphes3 for detector simulation.
- SUSY spectrm is calculated with SUSPECT and followed by SDECAY for the branching ratios and Prospino for calculating cross sections.

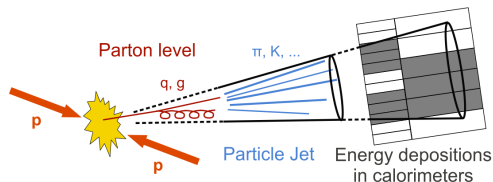
$$\begin{array}{llllll}
 \text{pp} & \rightarrow & \tilde{t}_1 \tilde{t}_1^* & \rightarrow & t \bar{t} \tilde{\chi}_2^0 \tilde{\chi}_2^0 & \rightarrow & t \bar{t} + 2Z + 2\tilde{\chi}_1^0 & \rightarrow & t/\bar{t} + \ell\ell + \cancel{p}_T + X \\
 \text{pp} & \rightarrow & \tilde{t}_1 \tilde{t}_1^* & \rightarrow & t \bar{b} \tilde{\chi}_2^0 \tilde{\chi}_1^- & \rightarrow & t \bar{b} + W^- Z + 2\tilde{\chi}_1^0 & \rightarrow & t + \ell\ell + \cancel{p}_T + X \\
 \text{pp} & \rightarrow & \tilde{t}_1 \tilde{t}_1^* & \rightarrow & t \bar{b} \tilde{\chi}_2^0 \tilde{\chi}_1^- & \rightarrow & t \bar{b} + W^- h + 2\tilde{\chi}_1^0 & \rightarrow & t + \ell\ell + \cancel{p}_T + X \\
 \text{pp} & \rightarrow & \tilde{b}_1 \tilde{b}_1^* & \rightarrow & t \bar{t} \tilde{\chi}_1^+ \tilde{\chi}_1^- & \rightarrow & t \bar{t} + W^+ W^- + 2\tilde{\chi}_1^0 & \rightarrow & t/\bar{t} + \ell\ell + \cancel{p}_T + X \\
 \text{pp} & \rightarrow & \tilde{b}_1 \tilde{b}_1^* & \rightarrow & t \bar{b} \tilde{\chi}_1^- \tilde{\chi}_2^0 & \rightarrow & t \bar{b} + W^- Z + 2\tilde{\chi}_1^0 & \rightarrow & t + \ell\ell + \cancel{p}_T + X.
 \end{array}$$

- Signature of interest: 1 tagged top + di-lepton + jets + \cancel{p}_T at 14 TeV LHC.
- For 8 TeV, small cross sections, absence of boost are limiting factors to this analysis.
- For this analysis, we use MADGRAPH to generate events, PYTHIA to shower and hadronize, FASTJET to reconstruct normal jets/Fat jets and Delphes3 for detector simulation.
- SUSY spectrm is calculated with SUSPECT and followed by SDECAY for the branching ratios and Prospino for calculating cross sections.
- Backgrounds : $t\bar{t} + n$ jets, $t\bar{t}Z$, $t\bar{t}W$ and tbW .
- Strategy to be employed : Use top tag + dileptonic M_{T2} .

$$\begin{array}{llllll}
 pp & \rightarrow & \tilde{t}_1 \tilde{t}_1^* & \rightarrow & t \bar{t} \tilde{\chi}_2^0 \tilde{\chi}_2^0 & \rightarrow & t \bar{t} + 2Z + 2\tilde{\chi}_1^0 & \rightarrow & t/\bar{t} + \ell\ell + \cancel{p}_T + X \\
 pp & \rightarrow & \tilde{t}_1 \tilde{t}_1^* & \rightarrow & t \bar{b} \tilde{\chi}_2^0 \tilde{\chi}_1^- & \rightarrow & t \bar{b} + W^- Z + 2\tilde{\chi}_1^0 & \rightarrow & t + \ell\ell + \cancel{p}_T + X \\
 pp & \rightarrow & \tilde{t}_1 \tilde{t}_1^* & \rightarrow & t \bar{b} \tilde{\chi}_2^0 \tilde{\chi}_1^- & \rightarrow & t \bar{b} + W^- h + 2\tilde{\chi}_1^0 & \rightarrow & t + \ell\ell + \cancel{p}_T + X \\
 pp & \rightarrow & \tilde{b}_1 \tilde{b}_1^* & \rightarrow & t \bar{t} \tilde{\chi}_1^+ \tilde{\chi}_1^- & \rightarrow & t \bar{t} + W^+ W^- + 2\tilde{\chi}_1^0 & \rightarrow & t/\bar{t} + \ell\ell + \cancel{p}_T + X \\
 pp & \rightarrow & \tilde{b}_1 \tilde{b}_1^* & \rightarrow & t \bar{b} \tilde{\chi}_1^- \tilde{\chi}_2^0 & \rightarrow & t \bar{b} + W^- Z + 2\tilde{\chi}_1^0 & \rightarrow & t + \ell\ell + \cancel{p}_T + X.
 \end{array}$$

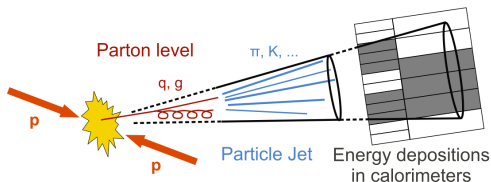
- Signature of interest: 1 tagged top + di-lepton + jets + \cancel{p}_T at 14 TeV LHC.
- For 8 TeV, small cross sections, absence of boost are limiting factors to this analysis.
- For this analysis, we use MADGRAPH to generate events, PYTHIA to shower and hadronize, FASTJET to reconstruct normal jets/Fat jets and Delphes3 for detector simulation.
- SUSY spectrm is calculated with SUSPECT and followed by SDECAY for the branching ratios and Prospino for calculating cross sections.
- Backgrounds : $t\bar{t} + n$ jets, $t\bar{t}Z$, $t\bar{t}W$ and tbW .
- Strategy to be employed : Use top tag + dileptonic M_{T2} .
- Literature on the use of top tagger in stop searches:
T Plehn et al. arXiv:1006.2833. D.E Kaplan et. al arXiv : 1205.5816. M. Perelstein et al. arXiv:1111.6594.
- Literature on the use of dileptonic M_{T2} : B. Tweedie et al. arXiv:1211.6106.





The Snowmass Accord:

- Simple to implement in expt and calculate theoretically.
- Defined at any order of perturbation theory and yields finite cross sections at all orders.
- Yields cross sections independent of hadronization procedure.
- IRC safe.



The Snowmass Accord:

- Simple to implement in expt and calculate theoretically.
- Defined at any order of perturbation theory and yields finite cross sections at all orders.
- Yields cross sections independent of hadronization procedure.
- IRC safe.

- Recombination Scheme : Distance measure: $d_{ij} = \min(p_{Ti}^{2p}, p_{Tj}^{2p}) \frac{\Delta R_{ij}^2}{R^2}$.

$$R = \sqrt{\eta^2 + \phi^2}$$

$$p=1 \rightarrow k_T; p=-1 \rightarrow \text{anti} - k_T; p=0 \rightarrow C/A.$$

- $k_T, C/A$: Cluster the softest particle first. anti - k_T : Cluster the hardest particles first.
- C/A being angular ordered is most suited to Jet Substructure.

Jet Substructures: Higgs tagger

- Digression: Jet Substructure : Higgs tagger

$$R_{b\bar{b}} \simeq 2 \frac{m_H}{p_T}, \quad (p_T \gg m_H)$$

- For $m_H \simeq 125$, $p_T > 250$ GeV, implies $R \simeq 1$
- As the boost increases, the jets get collimated.

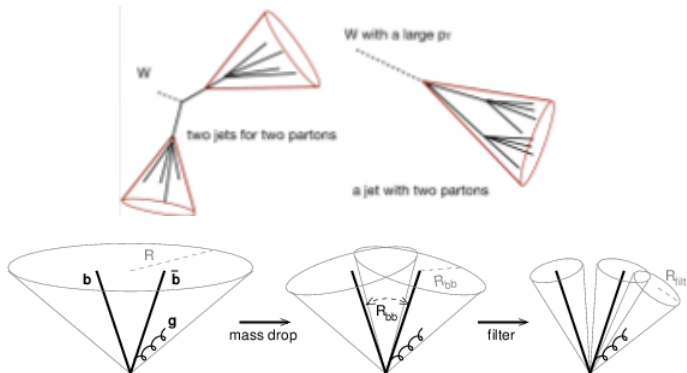


Jet Substructures: Higgs tagger

- Digression: Jet Substructure : Higgs tagger

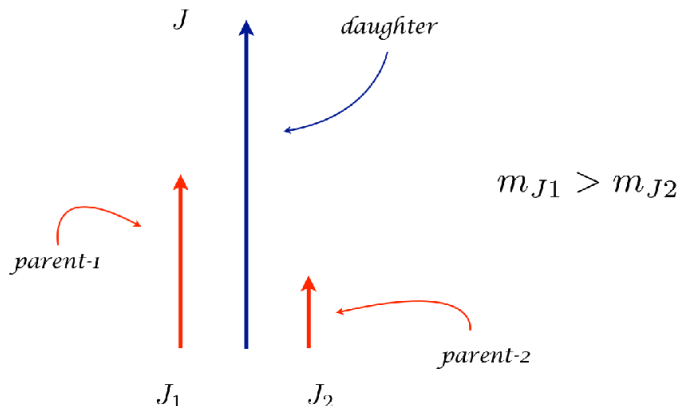
$$R_{b\bar{b}} \simeq 2 \frac{m_H}{p_T}, \quad (p_T \gg m_H)$$

- For $m_H \simeq 125$, $p_T > 250$ GeV, implies $R \simeq 1$
- As the boost increases, the jets get collimated.



- Butterworth, Rubin, Davison, Salam, 0802.2470.

*break a C/A b -jet J into two parents
by undoing its last stage of clustering*

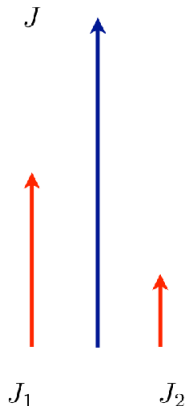


is J a suspect ?

check if

$$m_{J1} < 0.68 m_J$$

$$\min(p_{t1}^2, p_{t2}^2) \frac{\Delta R_{12}^2}{m_J^2} > (0.3)^2$$

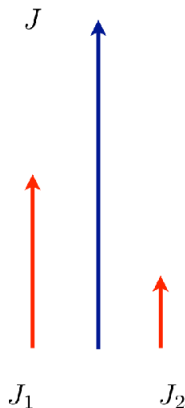


is J a suspect ?

check if

$$m_{J1} < 0.68 m_J$$

$$\min(p_{t1}^2, p_{t2}^2) \frac{\Delta R_{12}^2}{m_J^2} > (0.3)^2$$



if yes

J is at heavy particle threshold

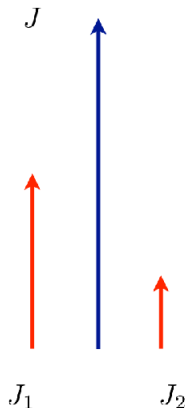
exit

is J a suspect ?

check if

$$m_{J1} < 0.68 m_J$$

$$\min(p_{t1}^2, p_{t2}^2) \frac{\Delta R_{12}^2}{m_J^2} > (0.3)^2$$



if no

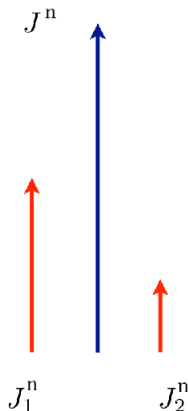
replace J by J_1

repeat

(Butterworth et al
0802.2470)

Filtering

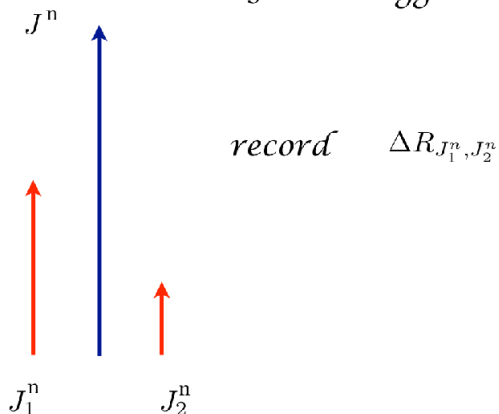
J^n is a Higgs candidate



(Butterworth et al
0802.2470)

Filtering

J^n is a Higgs candidate



Filtering

J^n is a Higgs candidate

J^n

de-cluster J^n completely

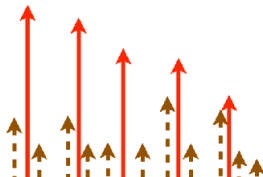


Filtering

re-cluster using

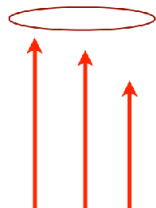
$$R_{\text{filt}} = \min \left(\frac{\Delta R_{J_1^n, J_2^n}}{2}, 0.3 \right)$$

Pt order the jets



Filtering

- *retain only three hardest component and combine. call it $H_{\text{iggs}} \text{ Jet}$*



- Cluster with C/A algorithm with a fat jet radius R .

- Cluster with C/A algorithm with a fat jet radius R .
- For each jet, decluster by undoing the last step of clustering. ($j \rightarrow j1, j2$) For the first decluster, if $p_T^{j1}/p_T^j < \delta_p$, throw p_T^{j1} , decluster p_T^{j2} and repeat. Typical values of $\delta_p = 0.19$, for $p_T \geq 1$ TeV.

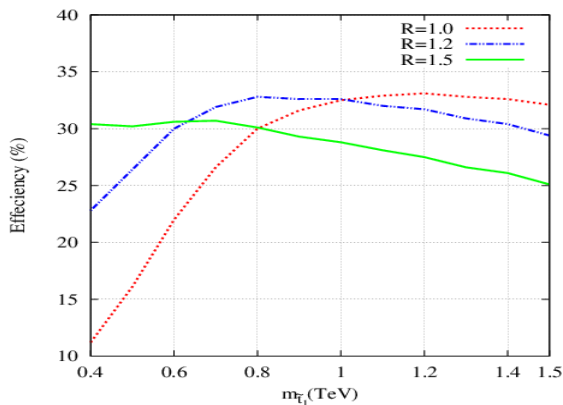
- Cluster with C/A algorithm with a fat jet radius R .
- For each jet, decluster by undoing the last step of clustering. ($j \rightarrow j1, j2$) For the first decluster, if $p_T^{j1}/p_T^j < \delta_p$, throw p_T^{j1} , decluster p_T^{j2} and repeat. Typical values of $\delta_p = 0.19$, for $p_T \geq 1$ TeV.
- Stop when either:
 - 1 $j1, j2$ both harder than δ_p .
 - 2 $j1, j2$ both softer than δ_p .
 - 3 $j1, j2$, too close (smaller than a parameter $\delta_r \simeq 0.10$).
 - 4 No other jet is left to decluster.

- Cluster with C/A algorithm with a fat jet radius R .
- For each jet, decluster by undoing the last step of clustering. ($j \rightarrow j1, j2$) For the first decluster, if $p_T^{j1}/p_T^j < \delta_p$, throw p_T^{j1} , decluster p_T^{j2} and repeat. Typical values of $\delta_p = 0.19$, for $p_T \geq 1$ TeV.
- Stop when either:
 - 1 $j1, j2$ both harder than δ_p .
 - 2 $j1, j2$ both softer than δ_p .
 - 3 $j1, j2$, too close (smaller than a parameter $\delta_r \simeq 0.10$).
 - 4 No other jet is left to decluster.
- For cases 2,3,4 deem j to be irreducible.
- For case 1 repeat till 3,4 total subjets are found.
- For 3 subjets, demand $145 \text{ GeV} < m_{\text{inv}}^{j1,j2,j3} < 205 \text{ GeV}$, and $65 \text{ GeV} < m_{\text{inv}}^{j2,j3} < 95 \text{ GeV}$
- Additionally to ensure proper W identification demand that the W helicity angle satisfies $\cos\theta_h < 0.7$
- To suppress the UE contamination, run the filtering algorithm.

Kaplan et al. -arXiv:0806.0848

Top tagging Efficiencies

Decay: $\tilde{t}_1 \rightarrow t\chi_2^0$. Fix $\chi_2^0 = 150$ GeV. Fat jet $p_T = 200$ GeV. Tag at least 1 top.

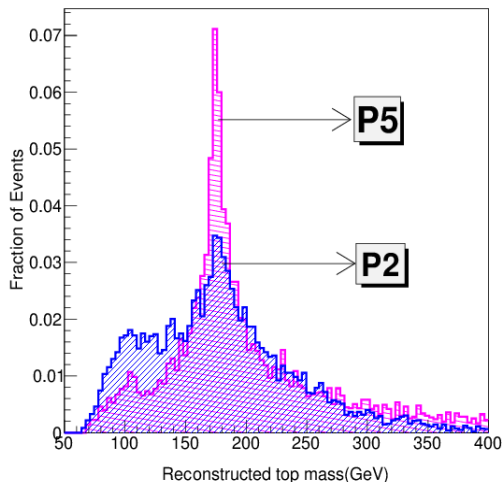


Optimal choice: $R=1.5$, $p_T = 200$ GeV.

Mass distributions for top tagging.

P2: $m_{\tilde{t}_1} \simeq 500$ GeV, $\chi_2^0 = 200$ GeV.

P5: $m_{\tilde{t}_1} \simeq 900$ GeV, $\chi_2^0 = 300$ GeV



- Note that all tops/jets are not tagged. Should we throw out these objects?
- Instead recluster untagged jets with anti- k_T algorithm with $R=0.5$.
- Identify the hadrons entering the fat jet, remove them from the jet list and run the anti- k_T algorithm on the rest, with $p_T^j = 50$ GeV
- Apply the dileptonic M_{T2} on the dileptonic system.

- The idea is to locate the end point in the mass distribution for decays with two branches of invisible particles.

-

$$M_T^2 \equiv m_\nu^2 + m_i^2 + 2(E_\nu E_i - \mathbf{v}_T \cdot \mathbf{p}_T),$$

- For W decaying invisibly, the end point of M_T is M_W

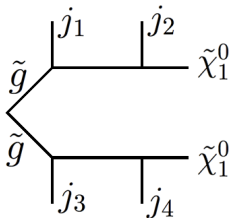
- The idea is to locate the end point in the mass distribution for decays with two branches of invisible particles.

•

$$M_T^2 \equiv m_\nu^2 + m_i^2 + 2(E_\nu E_i - \mathbf{v}_T \cdot \mathbf{p}_T),$$

.

- For W decaying invisibly, the end point of M_T is M_W



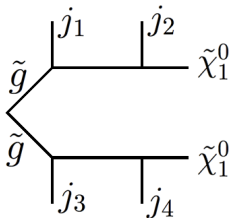
- The idea is to locate the end point in the mass distribution for decays with two branches of invisible particles.

•

$$M_T^2 \equiv m_\nu^2 + m_i^2 + 2(E_\nu E_i - \mathbf{v}_T \cdot \mathbf{p}_T),$$

.

- For W decaying invisibly, the end point of M_T is M_W



$$M_{T2}(\mathbf{v}_1, \mathbf{v}_2, \mathbf{p}_T) = \min [\max\{M_T(\mathbf{v}_1, \chi), M_T(\mathbf{v}_2, \chi)\}]$$

- minimization is performed over $\mathbf{p}_T^1 + \mathbf{p}_T^2 = \mathbf{p}_T$ where $\mathbf{p}_T^1, \mathbf{p}_T^2$ are all possible partitions.
- arXiv:0304226. A.Barr,C.Lester and P.Stephens

Lemma

When a pair of particles are produced, both with mass m_0 , and each parent decays to a visible system v and an invisible system i , then $M_{T2}(v_1, v_2, \not{p}_T, 0, 0) \leq m_0$.

Lemma

When a pair of particles are produced, both with mass m_0 , and each parent decays to a visible system v and an invisible system i , then $M_{T2}(v_1, v_2, \cancel{p}_T, 0, 0) \leq m_0$.



Lemma

When two particles are produced with different masses m_1 and m_2 and each parent decays to a visible system v and an invisible system i then $M_{T2}(v_1, v_2, \cancel{p}_T, 0, 0) \leq \max(m_1, m_2)$.

- [arXiv:0907.2713](https://arxiv.org/abs/0907.2713). A. Barr, C. Gwelan.

Lemma

When a pair of particles are produced, both with mass m_0 , and each parent decays to a visible system v and an invisible system i , then $M_{T2}(v_1, v_2, \cancel{p}_T, 0, 0) \leq m_0$.



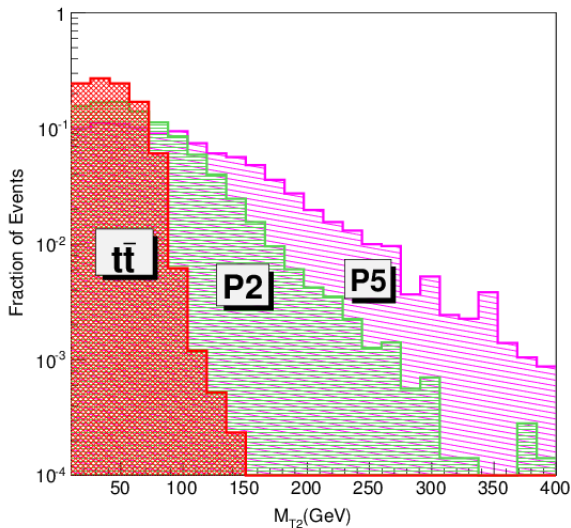
Lemma

When two particles are produced with different masses m_1 and m_2 and each parent decays to a visible system v and an invisible system i then $M_{T2}(v_1, v_2, \cancel{p}_T, 0, 0) \leq \max(m_1, m_2)$.

- [arXiv:0907.2713.A.Barr,C.Gwelan.](#)
- Caveat : Not always an **endpoint at parent mass**.
ISR, FSR, uncorrelated jets/leptons with \cancel{p}_T can spoil the party.
- In our case M_{T2} for $t\bar{t}$ is expected to have an end point at the mass of W.
- For signal since the mother particles from which these leptons come originate from χ_1^\pm, χ_2^0 , one expects an end point a higher values.

P2: $m_{\tilde{t}_1} \simeq 500$ GeV, $\chi_2^0 = 200$ GeV.

P5: $m_{\tilde{t}_1} \simeq 900$ GeV, $\chi_2^0 = 300$ GeV



- C1 : Demand at least two isolated leptons (electron and muon) with $p_T^\ell \geq 25$ GeV and $|\eta| \leq 3$.
- C2 : Consider M_{T2} defined as,

$$M_{T2}(\vec{p}_T^{\ell 1}, \vec{p}_T^{\ell 2}, \cancel{p}_T) = \min_{\cancel{p}_T = \cancel{p}_T^1 + \cancel{p}_T^2} \left[\max\{M_T(\vec{p}_T^{\ell 1}, \cancel{p}_T^1), M_T(\vec{p}_T^{\ell 2}, \cancel{p}_T^2)\} \right] > 125 \text{ GeV},$$

-
- C3 : Effective mass of the system $m_{\text{eff}} = \Sigma p_T^j + \Sigma p_T^\ell$.
- C4 : $\cancel{p}_T > 150$ GeV.
- C5 : At least 1 top tag in the system.

Results: Cut flow

Signal	Production Cross-section (fb)	Simulated events (in units of 10^4)	No. of events after the cut					Final Cross-section (in units of 10^{-2} fb)
			2l	M_{T2}	m_{eff}	\cancel{p}_T	top tag	
P1	1130	10	10573	821	339	267	55	62.2
P2	1130	10	11091	657	248	205	48	60.5
P3	135	5	8043	1132	712	645	153	41.3
P4	135	5	7713	1207	749	663	178	43.1
P5	27	5	8623	1720	1414	1322	295	15.9
P6	27	5	8543	1679	1343	1281	322	17.4

SM backgrounds	Production Cross-section (fb)	Simulated events (in units of 10^4)	No. of events after the cut					Final Cross-section (in units of 10^{-2} fb)
			C1	C2	C3	C4	C5	
$t\bar{t}$ + jets	918000	4320	1587596	601	39	29	4	8.5
$t\bar{t}W$	61000	600	215807	80	4	2	1	1.0
$t\bar{t}Z$	1121	7	6255	253	52	20	2	3.2
$t\bar{t}W$	769	5	4471	31	3	2	1	1.5
$t\bar{t}W^+W^-$	10	1	1588	33	14	13	6	0.6
$t\bar{t}t\bar{t}$	10	1	1781	31	14	10	4	0.4
Total Background								15.2

Define significance :

$$S = \frac{N_S}{\sqrt{N_B + (\kappa N_B)^2}} , \quad (1)$$

where N_S and N_B are the number of signal and background events respectively and κ is the measure of the systematic uncertainty.

	$m_{\tilde{t}_1}$ (GeV)	Signal(N_S) (Background(N_B))			Significance(S) for $\kappa = 10\%$ (30%, 50%)		
		10 fb ⁻¹	50 fb ⁻¹	100 fb ⁻¹	10 fb ⁻¹	50 fb ⁻¹	100 fb ⁻¹
P1	501.6	6.2(1.6)	31.1(8)	62.2(16)	4.9(4.6, 4.1)	10.8(8.4, 6.3)	14.4(9.9, 6.9)
P2	501.6	6.05(1.6)	30.2(8)	60.5(16)	4.7(4.5, 4.05)	10.6(8.3, 6.1)	14.1(9.6, 6.5)
P3	714.2	4.1(1.6)	20.7(8)	41.3(16)	3.2(3.0, 2.7)	7.0(5.6, 4.2)	9.6(6.6, 4.6)
P4	714.2	4.3(1.6)	21.55(8)	43.1(16)	3.6(3.3, 2.9)	7.4(5.9, 4.5)	9.9(6.8, 4.8)
P5	918.1	1.6(1.6)	7.9(8)	15.9(16)	1.3(1.2, 1.1)	2.7(2.1, 1.6)	3.7(2.5, 1.8)
P6	918.1	1.7(1.6)	8.7(8)	17.4(16)	1.3(1.2, 1.1)	2.9(2.3, 1.8)	4.0(2.8, 1.9)

Results in a simplified scenario

Consider the simplified models : $\tilde{t}_1 \rightarrow t\chi_2^0$, $\tilde{b}_1 \rightarrow t\chi_1^\pm$. $\chi_2^0 \rightarrow Z\chi_1^0$, $\chi_1^\pm \rightarrow W\chi_1^0$, with $\chi_1^0 = 50$ GeV

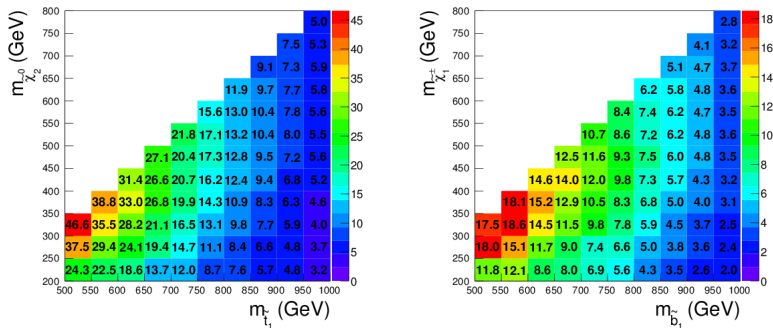


Figure: The signal significance at 100 fb⁻¹ in the \tilde{t}_1 - χ_2^0 plane (left panel) and \tilde{b}_1 - χ_1^\pm plane.

Conclusions

- The use of Jet Substructures and M_{T2} will have significant impacts in stop searches.
- In this study we studied the impact of the boosted stop strategy in a scenario where the stops were predominantly left handed.
- The optimized discovery reach of our strategy is about 900 GeV at 14 TeV center of mass energy with 100 fb^{-1} luminosity.

Conclusions

- The use of Jet Substructures and M_{T2} will have significant impacts in stop searches.
- In this study we studied the impact of the boosted stop strategy in a scenario where the stops were predominantly left handed.
- The optimized discovery reach of our strategy is about 900 GeV at 14 TeV center of mass energy with 100 fb^{-1} luminosity.



"One day, all of these will be supersymmetric phenomenology papers."